International Journal of Engineering

Journal Homepage: www.ije.ir

Fabrication of Pebax/4A Zeolite Nanocomposite Membrane to Enhance CO_2 Selectivity Compared to Pure O_2, N_2, and CH_4 Gases

S. M. Faghih, M. Salimi*, H. Mazaheri

Department of Chemical Engineering, Arak Branch, Islamic Azad University, Arak, Iran

P A P E R I N F O

Paper history:
Received 28 May 2022
Received in revised form 21 November 2022
Accepted 22 November 2022

Keywords:
CO_2 Separation
PEBAX
Membrane
Polymer Morphology
4A Zeolite Nanoparticles

A B S T R A C T

The separation of carbon dioxide is essential for the environment. Using membranes to separate this gas is economical, but the weakness in permeability and mechanical strength has prevented their commercialization. Robeson proved that permeability and selectivity have the opposite relationship and provided an upper limit for pairs of gases. Worth to be mentioned that any membrane placed above this limit could be commercialized. Scientists proposed mixed matrix membranes to overcome this problem. These membranes contain two phases, polymer, and inorganic. This research focuused on membrane technology and aimed to prepare a membrane that has a good performance for CO_2 separation and at the same time its cost is economical, so by adding a reasonable price zeolite available in the market named 4A to the Pebax1657 polymer and changing the operating conditions of the process, permeability and Selectivity was measured. Pebax polymer and 4A zeolite were selected as respectively the polymer and mineral phases for membrane fabrication. The fabricated membranes were evaluated by XRD, FT-IR, FE-SEM, BET, EDAX, TGA/DSC, and mechanical strength tests. Finally, the selectivity of CO_2 compared to N_2, O_2, and CH_4 improved by 53, 67, and 75%, respectively, and obtained a good position on the Robeson diagram.

***doi**: 10.5829/ije.2023.36.02b.19*

NOMENCLATURE

XRD	X-ray diffraction	a_s *BET*	Specific surface area based on BEt analysis ($m^2\ g^{-1}$)
FT-IR	Infrared Fourier transforms	*L*	Membrane thickness (cm)
FE-SEM	Field emission scanning electron microscopy	*V*	Tank volume after the membrane (cm^3)
BET	Brunauer-Emmett-Teller	P_o	Absolute input gas pressure (psia)
EDAX	X-ray energy scattering spectroscopy	*A*	Membrane area (cm^2)
TGA	Thermal balance analysis	V_m	Monolayer volume (cm^3(STP) g^{-1})
TPV	Total pore volume ($cm^3\ g^{-1}$)	*%Wt.*	Weight percent
P_A	Gas permeability A (Barrer)	*g*	Mass unit in grams
$\alpha_{A/B}$	The selectivity of A over B	*DMF*	Dimethylformamide solvent
µm	Micro metr (10^{-6} m)	*dP/dt*	Pressure changes in time (bar/s)

1. INTRODUCTION

The separation of carbon dioxide from the exhaust gases of chemical industries to preserve the environment and comply with standards has become an essential issue for industrial managers. When is not considered high purity in the separation of gases, membrane separation is the best technique [1,2]. The process of membrane separation requires small amount of energy [3-5].

Recently, researchers have for gases separation used Polyphosphazene, Polyamides, Cellulose acetate, Polyether-urethane, Polyamide-polyether-block copolymers, and Poly-vinylidene fluoride [2].

Lin et al. [6] concluded that using polar groups in polymers leads to a high selectivity for carbon dioxide

*Corresponding Author Institutional Email: m-salimi@iau-arak.ac.ir (S. M. Salimi)

Please cite this article as: S. M. Faghih, M. Salimi, H. Mazaheri, Fabrication of Pebax/4A Zeolite Nanocomposite Membrane to Enhance CO_2 Selectivity Compared to Pure O_2, N_2, and CH_4 Gases, ***International Journal of Engineering, Transactions B: Applications***, Vol. 36, No. 02, (2023), 408-419

compared to light gases. Copolymers containing ethylene oxides, such as polyether-block-amide or Pebax, are a very suitable proposal to achieve this aim [6]. Pebax is an elastomeric thermoplastic with a chemical structure as illustrated in Figure 1.

PA is an aliphatic polyamide that forms the hard part and PE polyether forms the soft part. The PA block provides mechanical resistance, and the passage of gas occurs from the PE phase. This polymer has good mechanical, and thermal stability [7].

Permeability and selectivity are two crucial actors in gas separation. Robeson reported a comprehensive analysis of gas pair permeability in polymer membranes. He proved that there is an inverse relationship between permeability and selectivity. In other words, these two factors have an opposite relationship [8]. Scientists are looking for a solution that increases permeability and selectivity simultaneously. One of their solutions is making composite membranes. These types of membranes include the polymer phase and filler phase [9-11]. With a combination of properties favorable to polymer membranes (high selectivity) and fillers (permeability and high mechanical stability), a stable and adjustable structure can be created, therewith expanding gas separation technology.

PEBA polymers provide the opportunity to produce membranes at a low cost. these polymers are commercially produced and can be converted into films with low thickness and excellent quality. The penetration, absorption, and permeability coefficients of films made from PEBA polymers vary due to their different chemical structure. Table 1 shows the chemical compositions and physical properties of some PEBA polymers. Among these polymers, the selectivity of

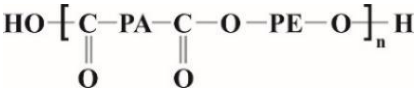

Figure 1. Chemical arrangement of PEBA polymers [7]

TABLE 1. Chemical compounds and physical properties of some PEBA polymers [7]

Type Polymer	Content PE (wt%)	Density (g/cm^3)	Melting temperature (°C)
2533	74.8 ,80	1.01	137, 126
3566	72.9 ,70	1.01	155, 142
4033	44,47	1.01	18, 159
5533	37.8	1.01	160
6333	42.2	-	170
1047	45	1.09	156
4011	43	1.14	201
1657	60	1.14	204

grade 1657 for CO_2 separation was the highest [12]. Zeolites have regular and tiny and controllable pores. They can act as a molecular sieve in the polymer membrane body [13]. Type A zeolite is a known synthetic example of the common compound Na1. $[AlO_2.SiO_2]12.27H_2O$ [14].

This type of zeolite has three different groups, 4A, 3A, and 5A, which differ in the type of cations present in their internal structure [15,16].

Often, zeolite type 4A (Figure 2) is used to absorb water and hazardous gases. But due to its pore size, it can play an essential role as a CO_2 molecule sifting [17,18]. These excellent properties help us to commercialize this nanocomposite. In Table 2, a summary of carbon dioxide separation research by nanocomposite membrane is compiled.

The objective of this research is to solve the weaknesses in permeability and selectivity which gained a suitable position in the Robeson diagram. As mentioned in the introduction, the Robson diagram is presented as an indicator for the commercialization of membranes, so the data were marked on the Robson diagram, and in this way, the evaluation of the commercialization of the nanocomposite membrane was done.

2. EXPERIMENTAL

2. 1. Materials Required For Membrane Preparation Pebax1657 was selected, made by French Arkema company with a density of 1.14 g/cm^3. Zeolite 4A powder made by Behdash Chemical Company of Iran was prepared. This material has a bulk density of 0.5 g/cm^3 and an average particle size of 250 to 500 nm. DMF solvent with a purity of 99% was sealed from Neutron Iran and standard hexane solvent was purchased from Merck (Darmstadt, Germany). Gases O_2, N_2, CH_4, and CO_2 with a purity of 99.9% were bought and used from Khorramshahr gas oxygen company.

2. 2. Devices Used In Membrane Preparation and Analysis XRD analysis with XRD Philips pw1730 device, FE-SEM analysis with TESCAN MIRA3 device, FT-IR analysis with Thermo company model AVATAR. T hedevice, BET analysis with particular surface

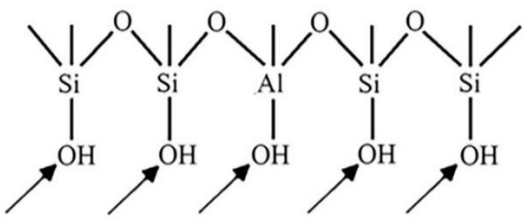

Figure 2. 4A zeolite structure [17]

TABLE 2. A selection of past research on membrane preparation with Pebax polymer and different nanoparticles

Ref.	Filler	Polymer	P_{CO2}	Selectivity
[24]	Zn/Co-ZIF	Pebax1657	102.5	16.4
[25]	Zeolite 13X	Pebax1657	168.59	45
[26]	ZIF-8	Pebax1074	144	72
[27]	ZnO	Pebax1074	152.27	13.52
[28]	TiO_2	Pebax1657	172	24.8
[29]	ZIF8	Pebax2533	727	63
[30]	Al_2O_3	Pebax1657	159.27	24.73
[31]	ZIF-8	Pebax1657/PE	758	16.1
[32]	DD3R	Pebax1074	188	38.5
[33]	ZIF-7	Pebax1657	150	40
[34]	NH2-CuBTC	Pebax1657	163	26.2
[35]	ZIF-7	Pebax1657	145	23
[36]	Zeolite NaY	Pebax1657	131.8	130.8
[37]	Zeolite NaX	Pebax1657/PES	45	121.5
[38]	ZIF-8	Pebax2533	1293	9
This work	4A	Pebax1657	115.5	CO_2/CH_4 32.3
This work	4A	Pebax1657	135.5	CO_2/O_2 20.53
This work	4A	Pebax1657	166.1	CO_2/N_2 75.19

measuring device: Belsorp mini II from Micro teach Bel Corp, Japan.

TGA/DSC analysis was done by TA company model Q600 device made in USA. To perform the mechanical resistance test was used Tensile Zwick device made in England, model CAT-350-56. The ultrasonic bath machine was manufactured by backer company vCLEAN1-L2. The thickness of the samples was measured by a digital thickness model GT-313-A1 made in Japan.

2. 3. Membrane Preparation And Synthesis Steps

Researchers have selected the membrane's thickness range between 60 and 120 µm [19-21]. Based on this, the amount of materials needed to prepare the membrane was roughly estimated according to the diameter of the petri dish and the thickness of 100 µm. Finally, after synthesizing the membranes, their thickness was measured using a thickness gauge. The nanocomposite was prepared by the solution mixing method.

To reach a concentration of 2.5 wt% of zeolite in the membrane, the first, 0.011 g of zeolite powder was placed at 70°C for 4 hours. In this way, the moisture was removed from the zeolite [22]. Then 12.076 g of DMF solvent (96.5%Wt. membrane) was added and placed on a magnetic stirrer at a temperature of 55°C for 4 hours [23].

The solution was placed in an ultrasonic bath for 15 minutes. In this way, we ensure the uniform distribution of nanoparticles and the removal of bubbles in the solution. This bath was set at a temperature of 50 °C, a frequency of 42 kHz, and a power of 50 W.

At this stage, the amount of 0.427 g of Pebax1657 granules was added to the solution and it was placed in an oil, and reflux bath at a temperature of 140 °C for 4 hours. To preserve the morphology of the nanocomposite and prevent damage to its structure, the bath was turned off 3 minutes before casting. In this way, the polymer was slightly cooled and ready for casting. Also, the glass petri dish was heated to 80 °C in the oven.

Then the obtained nanocomposite solution was poured into a Petri dish and immediately placed in the oven. The drying temperature and time were set at 40°C and 40 hours. During this time, the membrane was dehydrated. The Petri dish containing the membrane was removed from the oven, and a few drops of standard hexane solvent were poured on its surface.

So that its surface is free of any dust and undesirable particles. Then, for better drying and to ensure complete evaporation of the solvent, the petri dish containing the membrane was placed in a vacuum oven. The temperature of the oven was set at 45 °C. After 4 hours, the membrane was easily separated from the Petri dish and was ready for the permeability test.

In the same way, zeolite was made in the membrane for concentrations of 5, 8, 11.5, 16, and 22% Wt. The nanocomposite membranes prepared in this research were named Pebax1657/4A. Their thickness was measured and coded according to Table 3.

2. 4. Measurement of Permeability and Selectivity

The gas permeability measurement system was designed and built as a constant volume and according to Figure 3.

TABLE 3. Combination of polymer and nanoparticle in nanocomposite membranes

No	Pebax %Wt.	4A Zeolite wt%	ID
1	100	0	PA-0
2	97.5	2.5	PA-2.5
3	95	5	PA-5
4	92	8	PA-8
5	88.5	11.5	PA-11.5
6	84	16	PA-16
7	78	22	PA-22

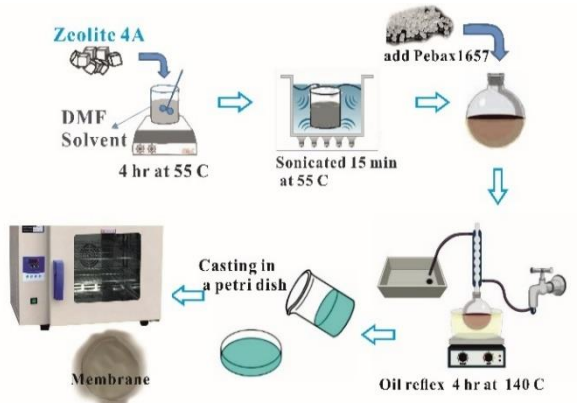

Figure 3. Nanocomposite membrane synthesis steps

This system can calculate gas permeability at different pressures and temperatures. The membrane cell is made of pure steel metal. To prevent gas leakage, rubber rings were installed on both sides of the membrane. The effective area of the membrane in this system is 17.71 cm^2.

Permeability experiments were performed at temperatures of 25, 35, 50, and 75 °C and pressures of 2, 5, 8 and 12 bars, each with three repetitions. Gas permeability was calculated using Equation (1) and reported in the Barrer unit.

$$P_{(Barrer)}=\frac{273.15\times10^{10}LV}{760\times76(AT\frac{P_0}{14.7})}\frac{dP}{dt} \quad (1)$$

1 Barrer $=10^{-10}$ cm^3 (STP)·cm/ (cm^2. s. cmHg)

In Equation (1), V (cm^3) is the volume of the reservoir after the cell, L (cm) is the thickness of the membrane, A (cm^2) is the effective area of the membrane, T (K) is the temperature, (psia) Po is the absolute pressure of the inlet gas and (bar/s) dP/dt is the pressure variation with time [39,40].

The selectivity of ideal gases was calculated using the equation 2 [41,42]. P_A and P_B are the permeability of gases A and B, respectively. The selectivity test results are discussed in the next sections; the selectivity expressed as ratio of P_A and P_B.

$$\alpha_{A/B}=\frac{P_A}{P_B} \quad (2)$$

Experimental set up for the gas permeabilty measurements is shown in Figure 4.

3. RESULTS AND DISCUSSION

3. 1. Analysis of X-ray Diffraction (XRD) XRD analysis was used to investigate the crystal structure of the synthesized membrane.

This analysis was performed from 10° to 80 ° with a step of 0.05° per second. The results of this analysis are shown in Figure 5. The zeolite phase is formed and has a

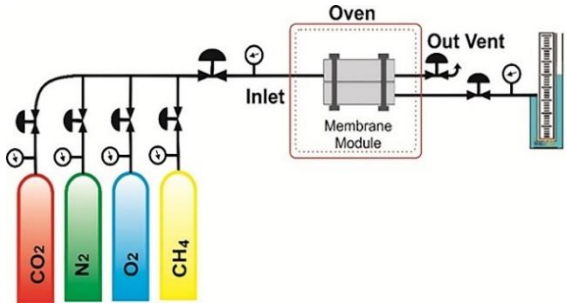

Figure 4. Permeability measurement system

crystal structure and favorable purity. The primary and significont peaks of the following particles after modification are related to X-ray reflection from planes 12.49, 20.09, 22, 27, 30, and 34 in the crystal structure of nanoparticles.

By comparing these figures with the results reported by other researchers [43], it can be said that the changes in the membrane structure are related to the addition of zeolite. In general, modifying the surface with non-crystalline agents reduces the crystallinity of the base particles. In this study, the size of the peaks in the central angles increased, which indicates an increase in membrane crystallinity and an increase in mechanical strength.

3. 2. Infrared Fourier Transforms (FT-IR) This analysis was performed on membranes from 600 cm^{-1} to 4000 cm^{-1}. As shown in Figure 6, the prominent peaks of pure Pebax1657 membrane around 1089 cm^{-1} wave number were attributed to stretching vibration (C-O-C) of ether group in soft parts. The height at 1635 cm^{-1} is the stretching vibrations of (O=C) carbonyl in (H-N-O=C). The rise in the wave number of 1729 cm^{-1} was attributed to another carbonyl group (C=O-O), both of which are in the complex phase.

The peak at 1538 cm^{-1} is related to N-H bending vibration in polyamide parts and the peak at 3292 cm^{-1} is related to stretching vibration (N-H). Also, the elevation of 2861 cm^{-1} and the prak of 1460 cm^{-1} was related to C-H stretching and bending vibration, respectively.

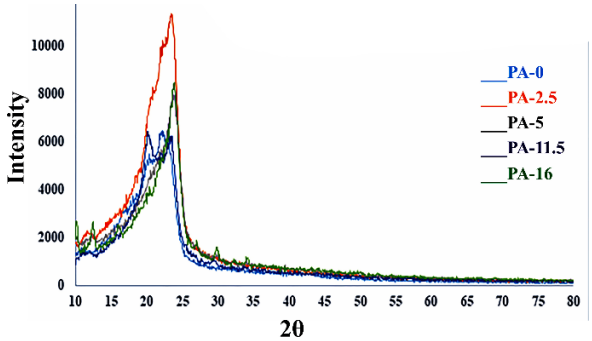

Figure 5. X-ray diffraction (XRD)

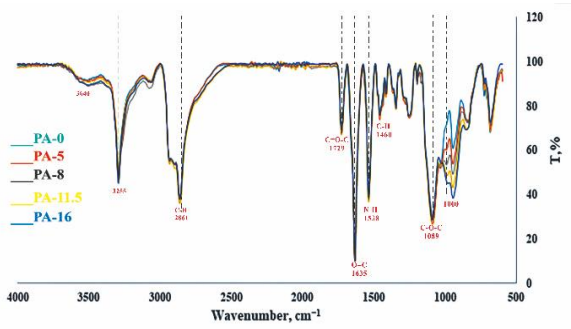

Figure 6. Fourier transform infrared spectroscopy

These results were in good agreement with another research [44]. In the spectrum of zeolite 4A, the broad absorption band in the wave number of 3255 cm^{-1} to 3640 cm^{-1} and the absorption band at 1650 cm^{-1} are related to hydroxyl (-OH) or silanol groups. Absorptions in wave number 1000 cm^{-1} are associated with O-Si or O-Al bending vibrations [45]. As the zeolite loading increased, the corresponding intensity of the peak at 3300 cm^{-1} also increased.

This significant change is attributed to filler phase loading. The absorption bands of zeolite overlap with the related bands in the Pebax spectrum. As the percentage of zeolite increases, the peak becomes higher at 1000 cm^{-1} due to the combined effect of Si-O or Al-O bonds in the zeolite. Finally, it can be said that the functional groups of Pebax and zeolite are placed next to each other with the help of physical bonds, and the formation of chemical bonds is ruled out.

3. 3. Imaging By Method Scanning Electron Microscopy (FE-SEM) The behavior of polymeric membranes depends on their structure and morphology. Any defect in the membrane structure can cause poor performance in permeability. Therefore, FE-SEM photography was carried out to examine the morphology of the membranes. Figure 7 shows the FE-SEM images of the fabricated membranes.

The pure Pebax membrane (PA-0) has a uniform surface and shows that its preparation method is suitable. According to these images, it can be seen that by adding nano zeolite to the polymer, the morphology of the membrane surface changes.

By increasing the amount of zeolite, the intensity of these changes also increases. Tendency to aggregation and clumping has been observed in the 16% zeolite loading sample. The imaging of the cross-section of the pure Pebax membrane with 8% and 11.5% loading is shown in Figure 7 (G, H and I), respectively; their thicknesses was 82.3, 83.95, and 91.1 µm.

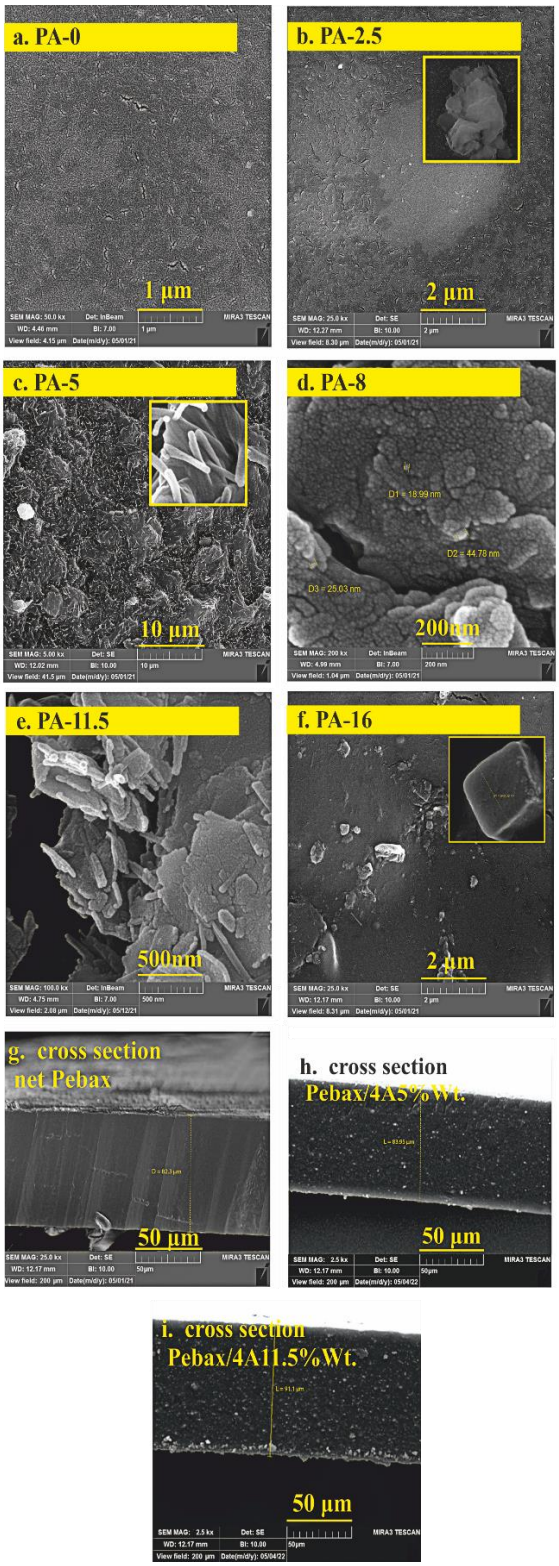

Figure 7. Scanning Electron Microscope (FE-SEM)

3. 4. X-ray Energy Scattering Spectroscopy (EDAX) Al, Si, and Na are the main elements of zeolite 4A, making up about 70 Wt.% of its atoms. The results of this analysis, according to Table 4, show that the percentage

of these atoms increases with an increase in the amount of zeolite in the membrane.

Also, Figures 8 and 9 show EDAX images for the the dispersion and proper distribution of elements on the surface of the membrane.

Still, the data of this analysis prove that the constructed membranes overcome this problem and the distribution of particles inside the polymer is uniform and acceptable. If the Si/Al ratio is less than 2, it indicates the hydrophilicity of the membrane [46]. In Table 4, this ratio for the PA-11.5 membrane is about 0.67. Membrane hydrophilicity can be an indicator of better CO_2 selectivity.

3. 5. Surface Measurement Specificity and Porosity (BET) BET analysis was performed to determine the physical properties of the synthesized membranes. In this specific surface area analysis, the total volume of specific pores, the size of the pore diameter and their distribution on the membrane surface were calculated.

Table 5 summarized that after loading nanoparticles, the specific surface area of the membrane increased by 46%. Increasing this parameter affects gas absorption.

Figure 10 shows the absorption-desorption diagram of nitrogen at a temperature of 77 °K of the PA-11.5 membrane. This sample showed the best performance in permeability and selectivity. This diagram is similar to the isotherm of the sixth type of the IUPAC standard. According to this standard, a diameter of less than 2 nm is classified as non-porous.

For a more detailed investigation, the size distribution of the pores on the surface of the membrane was calculated by the BJH method. The results for pore size distribution by BJH method of PA-11.5 membrane is shown in Figure 11. The maximum number of the graph is 1.2nm and 1.8nm, which means that the size of the holes is mostly the same.

3. 6. Thermogravimetric Analysis (TGA) In this analysis, heating rate of 10 °C/min was applied to the samples. The TGA curves of PA-0 and PA-11.5 membranes were drawn in Figure 12. The noticeable weight loss in the samples up to 206 °C is about 1%, caused by the evaporation of the remaining solvent in the polymer [47].

TABLE 4. The percentage of the number of central atoms of zeolite in the samples of the constructed membranes

Na	Si	Al	ID
0.0	0.02	0.02	PA-0
0.11	0.16	0.22	PA-2.5
0.27	0.23	0.34	PA-5
0.47	0.52	0.94	PA-8
0.76	0.48	0.71	PA-11.5
0.82	0.76	1.06	PA-16

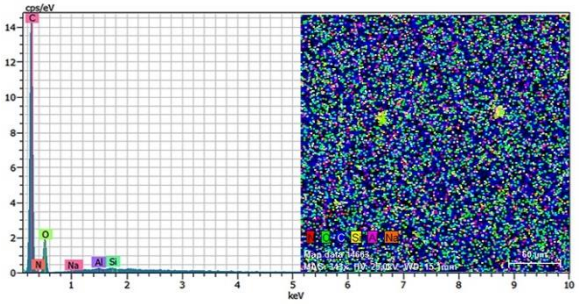

Figure 8. EDAX-Mapping PA-0

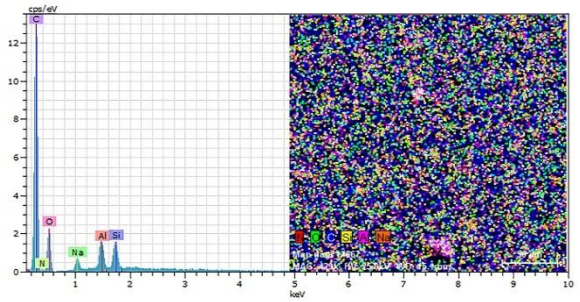

Figure 9. EDAX-Mapping PA-11.5

TABLE 5. BET analysis results

ID	TPV	$a_{s, BET}$	Vm
PA-0	0.0044627	4.596	1.056
PA-11.5	0.0086457	6.694	1.538

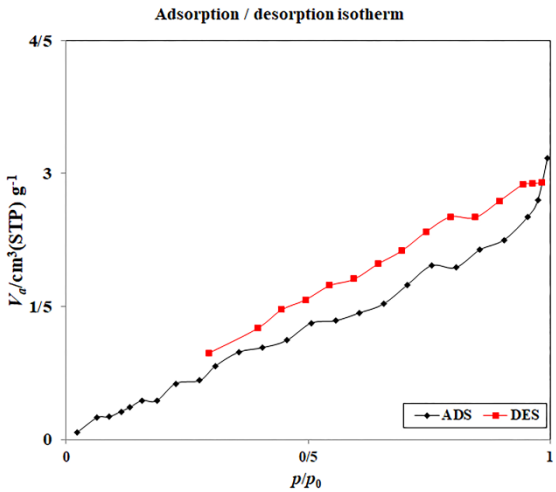

Figure 10. Isothermal absorption and desorption of nitrogen PA-11.5

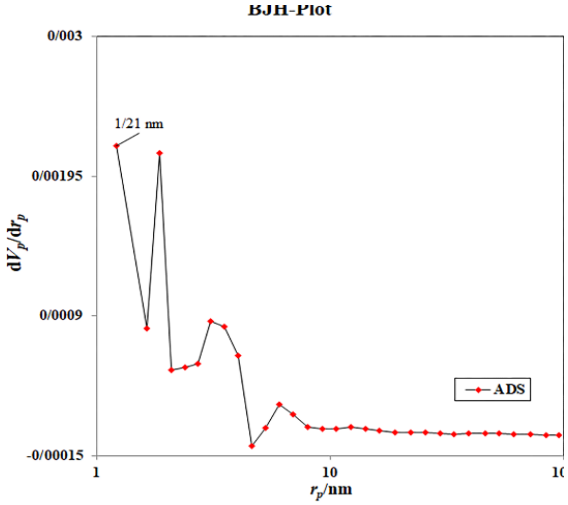

Figure 11. Pore size distribution by BJH method of PA-11.5 membrane

Weight loss in the PA-11.5 membrane started at about 328 °C. The reason is the beginning of the degradation of polymer chains. The DSC diagram shown the amount of energy required for this degradation. From about 361 to 446 °C, all polymer chains were destroyed. From about 450 °C, the polymer started to completely decompose and carbonate. After 525 °C, the weight did not change. But in the PA-0 membrane, the degradation started at 293 °C and at 450 °C, the chains were destroyed.

An increase in the destruction temperature in the nanocomposite membrane compared to the pure membrane is due to the physical bonds between nano zeolite and polymer. These bonds made the membrane strong. The formation of a strong covalent bond between them led to an increase in the energy required for destruction [48].

The DSC diagram shows the energy level needed to overcome these bonds. The TGA curve and the residual weight percentage confirm the presence of nano zeolite in the PA-11.5 membrane structure.

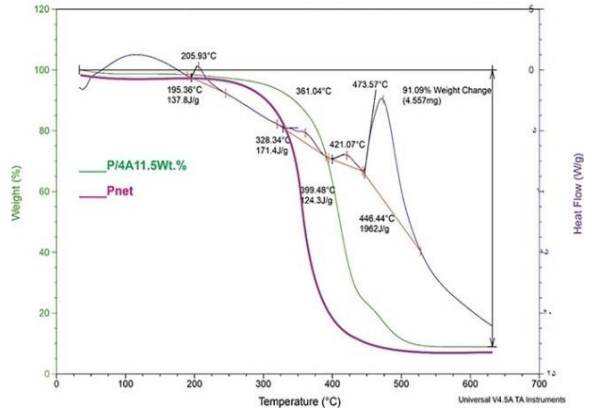

Figure 12. TGA/DSC analysis

3. 7. Analysis of Mechanical Strength

Mechanical strength analysis determines the tensile force a material can withstand before permanent damage. When a material is subjected to tensile force, it will withstand a certain amount of elongation before tearing. In this analysis, it was determined how strong the nanocomposite membrane is compared to the pure membrane.

The strip-shaped samples were placed between these two jaws of the machine and were drawn steadily at a speed of 5 mm/min. In this test, the temperature conditions and stretching rate remained constant. Table 6 shows the reaction of the manufactured membranes during the application of tensile force. In this table, it is shown that by addition of nanoparticles up to 11.5 wt%, the mechanical resistance of the composite membranes increased compared to the pure polymer membrane. The reason for that can be the proper physical bonding of nanoparticles and their coating by a polymer network. Also, this table shows that as the mass of particle increases, the membrane becomes denser. Excellent adhesion between nano zeolite and polymer, as well as their proper distribution on the surface of the membrane, increased the tensile strength.

The results of the EDAX analysis confirm that 4A particles are uniformly distributed in the polymer.The mechanical resistance of PA-16 and PA-22 membranes decreased. These two membranes cannot perform as well as the previous membranes. One of the reasons can be the clumping of nanoparticles in some places because clumping of nanoparticles causes their inability to interact with the polymer matrix and uneven stress distribution [48].

3. 8. Effect of Inlet Pressure

PA-11.5 nanocomposite membrane showed the best performance in permeability tests. For this reason, this membrane was chosen to investigate the effect of feed pressure on permeability and selectivity. By examining Figures 12, 13, and 14, the result of increasing the feed pressure on the permeability and selectivity of the membranes can be observed. As the pressure increased, the permeability of

TABLE 6. The mechanical performance of membranes

Loading Zeolite (Wt%)	Tensile strength (MPa)	Elastic modulus (MPa)	Elongation at break (%)
0	21.8	148.4	791 ± 2
2.5	23.1	135.3	812± 5
5	26.7	128.6	641 ± 5
8.5	29.3	118.5	598 ± 3
11.5	34.5	116.1	478 ± 3
16	19.9	95.8	251± 5
22.5	12.7	83.2	141 ± 5

CO_2 increased dramatically. at the same time, the permeability of other gases increased less. An increase in CO_2 permeability at higher pressures can be due to an increase in solubility due to the absorption of more CO_2 molecules in the polymer network [49]. Figure 12 demonstrates TGA/DSC analysis of the fabricated membrane

With an increase in pressure, the number of CO_2 molecules on the surface of the membrane increases. This increase creates a hydrogen bond between the O atom corresponding to the CO_2 molecule and the H of the amide groups on the surface of the polymer, for this reason, the selectivity of this gas increases. [6, 50]. Figure 13 shows the Robeson constraint chart for the selectivity of CO_2/CH_4 and CO_2/N_2 for the different Pebax 1657, Pebax 1657/4A and Pebax 1657/4A 11.5wt% of nanoparticles. In Figure 13, the performance of the optimized membrane in this study was marked on the Robeson diagram. This figure shows that the membrane was placed on the Robeson line. As a result, it can be considered a suitable option for separating carbon dioxide gas from other light gases in chemical industries.

3. 9. Effect of Operating Temperature The kinetic energy of gas molecules at high temperatures destroyed some of the polymer chains ,and the polymer network became more flexible. This flexibility in the polymer network can increase the molecular free volume coefficient in the membrane. Therefore, the membrane permeability increased, but the selectivity significantly decreased [51]. The reason for that can be the decrease in the solubility of CO_2 at temperatures higher than 35°C. If the solubility coefficient decreases, the selectivity of CO_2 also decreases compared to other gases [6]. Figure 14 shows CO_2 / N_2 selectivity at different temperatures and pressures; while Figure 15 illustrates CO_2 / CH_4 selectivity at different temperatures and pressures. In addition, the selectivity of CO_2/O_2 at different temperatures and pressures is shown in Figure 16.

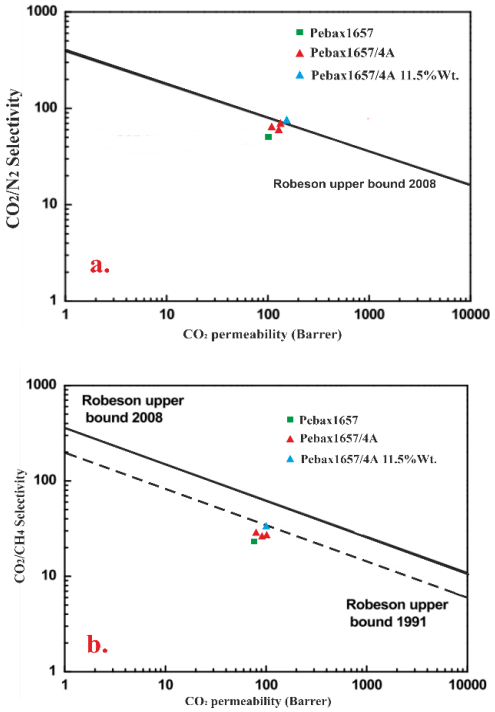

Figure 13. Robeson constraint chart

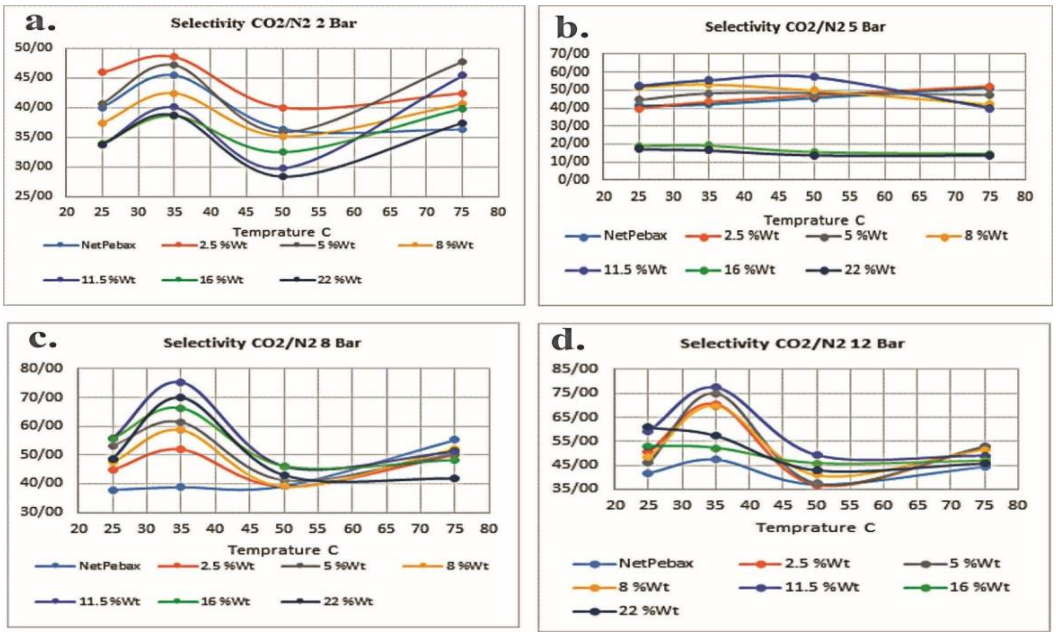

Figure 14. CO_2 / N_2 selectivity in different temperatures and pressures

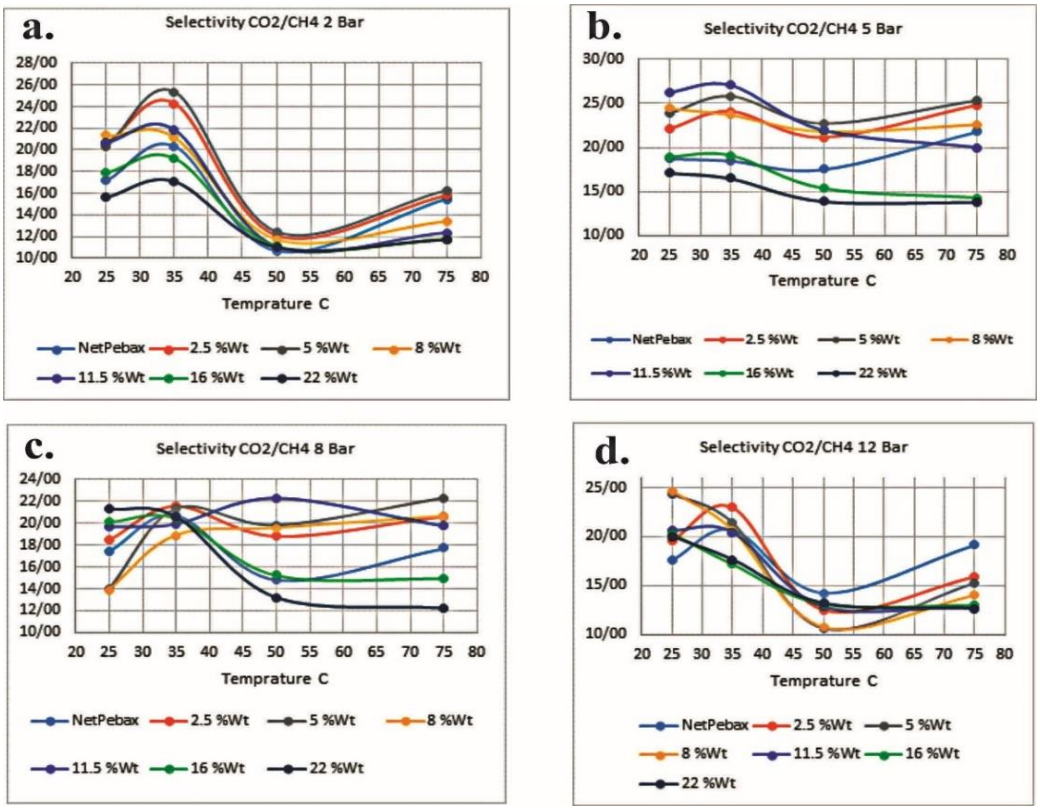

Figure 15. CO_2 / CH_4 selectivity in different temperatures and pressures

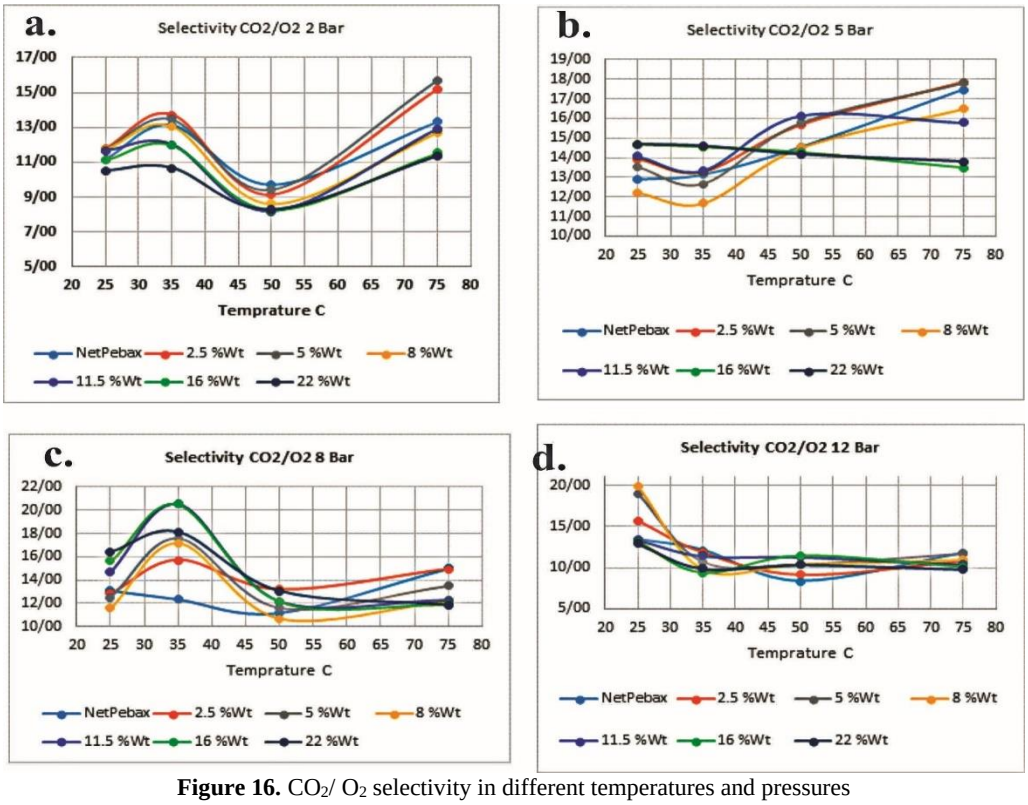

Figure 16. CO_2/ O_2 selectivity in different temperatures and pressures

4. CONCLUSION

In this research, Pebax 1657/4A zeolite nanocomposite membranes were prepared by casting and solvent evaporation. Their performance was investigated under operating conditions of 25 to 75 °C and pressures of 2 to 12 Bar for separating CO_2 gas relative to N_2, CH_4, and O_2. The results of FT-IR test denied the formation of a chemical bond between zeolite and polymer. FE-SEM images and EDAX analysis showed that the nano zeolites were well dispersed in the polymer, and a suitable nanocomposite membrane structure was obtained.

The TGA/DSC test showed that the thermal resistance of the nanocomposite membrane has increased compared to the polymer membrane. It also proved physical solid bonds between nano zeolite and polymer. CO_2 selectivity increased with increasing operating pressure. An increase in the operating temperature causes a significant increase in the permeability of gases due to an increase in their molecular kinetic energy and the polymer chains becoming more flexible. But the selectivity was significantly reduced. BET test showed that the pore size of nanocomposite membranes is less than 2 nm. This size is proportional to CO_2 molecules. These molecules can pass with less resistance than the pure polymeric membrane. Nanoparticle loading reduces the density of polymer chains and weakens the hydrogen bond between them. This factor increases the free volume between molecules and increases permeability.

The results of the gas permeability test showed that the best result was obtained at a temperature of 35 °C by adding 11.5% Wt. of zeolite to the polymer membrane. The best selectivity of CO_2 against N_2, O_2, and CH_4 was obtained at 12, 8, and 5 bar pressures, respectively.

Finally, the selectivity of the Pebax1657/4A nanocomposite membrane was 64, 67, and 45% better than pure Pebax in the mentioned operating conditions, respectively. As mentioned in the introduction, Robeson presented a limit in the permeability selectivity diagram, which was called Robeson's upper limit. The closer the polymer membrane is to this upper limit of the graph, the more suitable it is for industrialization.

Nowadays, the elimination of these gases has become a vital issue for researchers so that they can prevent the excessive heating of the earth.

5. REFERENCES

1. Othman, F.E.C., Yusof, N., Petrů, M., Nordin, N.A.H.M., Hamid, M.F., Ismail, A.F., Rushdan, A.I. and Hassan, S.A., "Polyethyleneimine-impregnated activated carbon nanofiber composited graphene-derived rice husk char for efficient post-combustion CO_2 capture", ***Nanotechnology Reviews***, Vol. 11, No. 1, (2022), 926-944. https://doi.org/10.1515/ntrev-2022-0055
2. A. Brunettia, F.S., G. Barbieria, E. Driolia,b, "Membrane technologies for CO_2 separation", ***Journal of Membrane Science***, Vol. 359, No. 1-2, (2010), 115-125. https://doi.org/10.1016/j.memsci.2009.11.040
3. Aghanezhad, M., Shafaghat, R., Alamian, R., Seyedi, S.M.A. and Raji Asadabadi, M.J., "Experimental study on performance assessment of hydraulic power take-off system in centipede wave energy converter considering caspian sea wave characteristics", ***International Journal of Engineering, Transactions B: Applications***, Vol. 35, No. 5, (2022), 883-899. https://doi.org/10.5829/ije.2022.35.05b.17
4. Jahanbakhsh, A., Hosseini, M., Jahanshahi, M. and Amiri, A., "Extraction of catechin as a flavonoid compound via molecularly imprinted polymers", ***International Journal of Engineering, Transactions B: Applications***, Vol. 35, No. 5, (2022), 988-995. https://doi.org/10.5829/ije.2022.35.08b.05
5. Mirhosseini, N., Davarnejad, R., Hallajisani, A., Cano-europa, E. and Tavakoli, O., "Sugarcane molasses as a cost-effective carbon source on arthrospira maxima growth by taguchi technique", ***International Journal of Engineering, Transactions C: Aspects***, Vol. 35, No. 3, (2022), 510-516. https://doi.org/10.5829/ije.2022.35.03C.13
6. Lin, H., Freeman, B.D., Kalakkunnath, S. and Kalika, D.S., "Effect of copolymer composition, temperature, and carbon dioxide fugacity on pure-and mixed-gas permeability in poly (ethylene glycol)-based materials: Free volume interpretation", ***Journal of Membrane Science***, Vol. 291, No. 1-2, (2007), 131-139. https://doi.org/10.1016/j.memsci.2007.01.001
7. Sheth, J.P., Xu, J. and Wilkes, G.L., "Solid state structure–property behavior of semicrystalline poly(ether-block-amide) pebax® thermoplastic elastomers", ***Polymer***, Vol. 44, No. 3, (2003), 743-756. https://doi.org/10.1016/S0032-3861(02)00798-X
8. Robeson, L.M., "The upper bound revisited", ***Journal of Membrane Science***, Vol. 320, No. 1-2, (2008), 390-400. https://doi.org/10.1016/j.memsci.2008.04.030
9. Kianfar, F. and Kianfar, E., "Synthesis of isophthalic acid/aluminum nitrate thin film nanocomposite membrane for hard water softening", ***Journal of Inorganic and Organometallic Polymers and Materials***, Vol. 29, No. 6, (2019), 2176-2185. https://doi.org/10.1007/s10904-019-01177-1
10. Kianfar, E., Salimi, M., Kianfar, F., Kianfar, M. and Razavikia, S.A.H., " CO_2/N_2 separation using polyvinyl chloride iso-phthalic acid/aluminium nitrate nanocomposite membrane", ***Macromolecular Research***, Vol. 27, No. 1, (2019), 83-89. https://doi.org/10.1007/s13233-019-7009-4
11. Salimi, M., Pirouzfar, V. and Kianfar, E., "Novel nanocomposite membranes prepared with pvc/abs and silica nanoparticles for C_2H_6/CH_4 separation", ***Polymer Science, Series A***, Vol. 59, No. 4, (2017), 566-574. https://doi.org/10.1134/S0965545X17040071
12. Embaye, A.S., Martínez-Izquierdo, L., Malankowska, M., Téllez, C. and Coronas, J., "Poly(ether-block-amide) copolymer membranes in CO_2 separation applications", ***Energy & Fuels***, Vol. 35, No. 21, (2021), 17085-17102. https://doi.org/10.1021/acs.energyfuels.1c01638
13. Salimi, M., Pirouzfar, V. and Kianfar, E., "Enhanced gas transport properties in silica nanoparticle filler-polystyrene nanocomposite membranes", ***Colloid and Polymer Science***, Vol. 295, No. 1, (2017), 215-226. https://doi.org/10.1007/s00396-016-3998-0
14. Padhi, P., Rout, S. and Panda, D., "Effect of modification of zeolite a using sodium carboxymethylcellulose (CMC)", ***Bulgarian Chemical Communications,*** Vol. 46, No.4, (2014), 777-783.

15. Shariatzadeh, S.M.R., Salimi, M., Fathinejad, H. and Hassani Joshaghani, A., "Nanostructured α-Fe_2O_3: Solvothermal synthesis, characterization, and effect of synthesis parameters on structural properties", ***International Journal of Engineering, Transactions C: Aspects***, Vol. 35, No. 6, (2022), 1186-1192. https://doi.org/10.5829/ije.2022.35.06c.10
16. Andami, P., Zinatizadeh, A.A., Feyzi, M., Zangeneh, H., Azizi, S., Norouzi, L. and Maaza, M., "Optimization of biodiesel production from sunflower oil transesterification using Ca-k/Al_2O_3 nanocatalysts", ***International Journal of Engineering, Transactions B: Applications***, Vol. 35, No. 2, (2022), 351-359. https://doi.org/10.5829/ije.2022.35.02b.11
17. Ahmad, J. and Hägg, M.-B., "Preparation and characterization of polyvinyl acetate/zeolite 4a mixed matrix membrane for gas separation", ***Journal of Membrane Science***, Vol. 427, (2013), 73-84. https://doi.org/10.1016/j.memsci.2012.09.036
18. Chung, T.-S., Jiang, L.Y., Li, Y. and Kulprathipanja, S., "Mixed matrix membranes (MMMS) comprising organic polymers with dispersed inorganic fillers for gas separation", ***Progress in Polymer Science***, Vol. 32, No. 4, (2007), 483-507. https://doi.org/10.1016/j.progpolymsci.2007.01.008
19. Saeedi Dehaghani, A.H. and Pirouzfar, V., "Preparation of high-performance membranes derived from poly (4-methyl-1-pentene)/zinc oxide particles", ***Chemical Engineering & Technology***, Vol. 40, No. 9, (2017), 1693-1701. https://doi.org/10.1002/ceat.201600693
20. Suhas, D.P., Aminabhavi, T.M. and Raghu, A.V., "Para-toluene sulfonic acid treated clay loaded sodium alginate membranes for enhanced pervaporative dehydration of isopropanol", ***Applied Clay Science***, Vol. 101, (2014), 419-429. https://doi.org/10.1016/j.clay.2014.08.017
21. Dharupaneedi, S.P., Anjanapura, R.V., Han, J.M. and Aminabhavi, T.M., "Functionalized graphene sheets embedded in chitosan nanocomposite membranes for ethanol and isopropanol dehydration via pervaporation", ***Industrial & Engineering Chemistry Research***, Vol. 53, No. 37, (2014), 14474-14484. https://doi.org/10.1021/ie502751h
22. Kianfar, E., Pirouzfar, V. and Sakhaeinia, H., "An experimental study on absorption/stripping CO_2 using mono-ethanol amine hollow fiber membrane contactor", ***Journal of the Taiwan Institute of Chemical Engineers***, Vol. 80, (2017), 954-962. https://doi.org/10.1016/j.jtice.2017.08.017
23. Saeedi Dehaghani, A.H., Pirouzfar, V. and Alihosseini, A., "Novel nanocomposite membranes-derived poly(4-methyl-1-pentene)/functionalized titanium dioxide to improve the gases transport properties and separation performance", ***Polymer Bulletin***, Vol. 77, No. 12, (2020), 6467-6489. https://doi.org/10.1016/j.jtice.2017.08.017
24. Cheng, J., Wang, Y., Liu, N., Hou, W. and Zhou, J., "Enhanced CO_2 selectivity of mixed matrix membranes with carbonized zn/co zeolitic imidazolate frameworks", ***Applied Energy***, Vol. 272, (2020), 115179. https://doi.org/10.1016/j.apenergy.2020.115179
25. Asghari, M., Mosadegh, M. and Harami, H.R., "Supported peba-zeolite 13x nano-composite membranes for gas separation: Preparation, characterization and molecular dynamics simulation", ***Chemical Engineering Science***, Vol. 187, (2018), 67-78. https://doi.org/10.1016/j.apenergy.2020.115179
26. Atash Jameh, A., Mohammadi, T. and Bakhtiari, O., "Preparation of pebax-1074/modified zif-8 nanoparticles mixed matrix membranes for CO_2 removal from natural gas", ***Separation and Purification Technology***, Vol. 231, (2020), 115900. https://doi.org/10.1016/j.seppur.2019.115900
27. Azizi, N., Mohammadi, T. and Behbahani, R.M., "Synthesis of a pebax-1074/zno nanocomposite membrane with improved CO_2 separation performance", ***Journal of Energy Chemistry***, Vol. 26, No. 3, (2017), 454-465. https://doi.org/10.1016/j.seppur.2019.115900
28. Azizi, N., Isanejad, M., Mohammadi, T. and Behbahani, R.M., "Effect of tio2 loading on the morphology and CO_2/ CH_4 separation performance of pebax-based membranes", ***Frontiers of Chemical Science and Engineering***, Vol. 13, No. 3, (2019), 517-530. https://doi.org/10.1016/j.seppur.2019.115900
29. Deng, J., Dai, Z. and Deng, L., "Effects of the morphology of the zif on the CO_2 separation performance of mmms", ***Industrial & Engineering Chemistry Research***, Vol. 59, No. 32, (2020), 14458-14466. https://doi.org/10.1021/acs.iecr.0c01946
30. Farashi, Z., Azizi, S., Arzhandi, M.R.-D., Noroozi, Z. and Azizi, N., "Improving CO_2/ CH_4 separation efficiency of pebax-1657 membrane by adding Al_2O_3 nanoparticles in its matrix", ***Journal of Natural Gas Science and Engineering***, Vol. 72, No., (2019), 103019. https://doi.org/10.1016/j.jngse.2019.103019
31. Jomekian, A., Behbahani, R.M., Mohammadi, T. and Kargari, A., "CO_2/ CH_4 separation by high performance co-casted zif-8/pebax 1657/pes mixed matrix membrane", ***Journal of Natural Gas Science and Engineering***, Vol. 31, (2016), 562-574. https://doi.org/10.1016/j.jngse.2016.03.067
32. Karamouz, F., Maghsoudi, H. and Yegani, R., "Synthesis of high-performance pebax®-1074/dd3r mixed-matrix membranes for CO_2/ CH_4 separation", ***Chemical Engineering & Technology***, Vol. 41, No. 9, (2018), 1767-1775. https://doi.org/10.1002/ceat.201800087
33. Khoshkharam, A., Azizi, N., Behbahani, R.M. and Ghayyem, M.A., "Separation of CO_2 from CH_4 using a synthesized pebax-1657/zif-7 mixed matrix membrane", ***Petroleum Science and Technology***, Vol. 35, No. 7, (2017), 667-673. https://doi.org/10.1080/10916466.2016.1273242
34. Khosravi, T., Omidkhah, M., Kaliaguine, S. and Rodrigue, D., "Amine-functionalized cubtc/poly (ether-b-amide-6)(pebax® mh 1657) mixed matrix membranes for CO_2/ CH_4 separation", ***The Canadian Journal of Chemical Engineering***, Vol. 95, No. 10, (2017), 2024-2033. https://doi.org/10.1002/cjce.22857
35. Li, T., Pan, Y., Peinemann, K.-V. and Lai, Z., "Carbon dioxide selective mixed matrix composite membrane containing zif-7 nano-fillers", ***Journal of Membrane Science***, Vol. 425, (2013), 235-242. https://doi.org/10.1002/cjce.22857
36. Zheng, Y., Wu, Y., Zhang, B. and Wang, Z., "Preparation and characterization of CO_2-selective pebax/nay mixed matrix membranes", ***Journal of Applied Polymer Science***, Vol. 137, No. 9, (2020), 48398. https://doi.org/10.1002/cjce.22857
37. Zarshenas, K., Raisi, A. and Aroujalian, A., "Mixed matrix membrane of nano-zeolite nax/poly (ether-block-amide) for gas separation applications", ***Journal of Membrane Science***, Vol. 510, (2016), 270-283. https://doi.org/10.1002/cjce.22857
38. Nafisi, V. and Hägg, M.-B., "Development of dual layer of zif-8/pebax-2533 mixed matrix membrane for CO_2 capture", ***Journal of Membrane Science***, Vol. 459, (2014), 244-255. https://doi.org/10.1002/cjce.22857
39. Hosseinzadeh Beiragh, H., Omidkhah, M., Abedini, R., Khosravi, T. and Pakseresht, S., "Synthesis and characterization of poly (ether-block-amide) mixed matrix membranes incorporated by nanoporous zsm-5 particles for CO_2/ch4 separation", ***Asia-Pacific Journal of Chemical Engineering***, Vol. 11, No. 4, (2016), 522-532. https://doi.org/10.1002/cjce.22857
40. mousavian, S., Faravar, P., Zarei, Z., azimikia, R., Ghasemi Monjezi, M. and kianfar, E., "Modeling and simulation absorption of CO_2 using hollow fiber membranes (HFM) with mono-ethanol amine with computational fluid dynamics", ***Journal of Environmental Chemical Engineering***, Vol. 8, No. 4, (2020), 103946. https://doi.org/10.1016/j.jece.2020.103946
41. Kianfar, E. and Cao, V., "Polymeric membranes on base of polymethyl methacrylate for air separation: A review", ***Journal***

of Materials Research and Technology, Vol. 10, (2021), 1437-1461. https://doi.org/10.1016/j.jmrt.2020.12.061

42. Kianfar, E., Pirouzfar, V. and Sakhaeinia, H., "An experimental study on absorption/stripping CO_2 using mono-ethanol amine hollow fiber membrane contactor", ***Journal of the Taiwan Institute of Chemical Engineers***, Vol. 80, No., (2017), 954-962. https://doi.org/10.1016/j.jtice.2017.08.017
43. Khoramzadeh, E., Mofarahi, M. and Lee, C.-H., "Equilibrium adsorption study of CO_2 and N2 on synthesized zeolites 13x, 4a, 5a, and beta", ***Journal of Chemical & Engineering Data***, Vol. 64, No. 12, (2019), 5648-5664. https://doi.org/10.1021/acs.jced.9b00690
44. Surya Murali, R., Ismail, A.F., Rahman, M.A. and Sridhar, S., "Mixed matrix membranes of pebax-1657 loaded with 4a zeolite for gaseous separations", ***Separation and Purification Technology***, Vol. 129, (2014), 1-8. https://doi.org/10.1016/j.seppur.2014.03.017
45. Zou, W., Bai, H., Zhao, L., Li, K. and Han, R., "Characterization and properties of zeolite as adsorbent for removal of uranium(vi) from solution in fixed bed column", ***Journal of Radioanalytical and Nuclear Chemistry***, Vol. 288, No. 3, (2011), 779-788. https://doi.org/10.1016/j.seppur.2014.03.017
46. Castillo, J.M., Silvestre-Albero, J., Rodriguez-Reinoso, F., Vlugt, T.J. and Calero, S., "Water adsorption in hydrophilic zeolites: Experiment and simulation", ***Physical Chemistry Chemical Physics***, Vol. 15, No. 40, (2013), 17374-17382.
47. Azizi, N., Isanejad, M., Mohammadi, T. and Behbahani, R.M., "Effect of TiO_2 loading on the morphology and CO_2/ CH_4 separation performance of pebax-based membranes", ***Frontiers of Chemical Science and Engineering***, Vol. 13, No. 3, (2019), 517-530. https://doi.org/10.1007/s11705-018-1781-0
48. Basu, S., Cano-Odena, A. and Vankelecom, I.F.J., "Mof-containing mixed-matrix membranes for CO_2/CH_4 and CO_2/N_2 binary gas mixture separations", ***Separation and Purification Technology***, Vol. 81, No. 1, (2011), 31-40. https://doi.org/10.1016/j.seppur.2011.06.037
49. Sridhar, S., Suryamurali, R., Smitha, B. and Aminabhavi, T.M., "Development of crosslinked poly(ether-block-amide) membrane for CO_2/CH_4 separation", ***Colloids and Surfaces A: Physicochemical and Engineering Aspects***, Vol. 297, No. 1, (2007), 267-274. https://doi.org/10.1016/j.colsurfa.2006.10.054
50. Saeedi Dehaghani, A.H., Pirouzfar, V. and Alihosseini, A., "Novel nanocomposite membranes-derived poly(4-methyl-1-pentene)/functionalized titanium dioxide to improve the gases transport properties and separation performance", ***Polymer Bulletin***, Vol. 77, No. 12, (2020), 6467-6489. https://doi.org/10.1016/j.colsurfa.2006.10.054
51. Rahman, M.M., Shishatskiy, S., Abetz, C., Georgopanos, P., Neumann, S., Khan, M.M., Filiz, V. and Abetz, V., "Influence of temperature upon properties of tailor-made pebax® mh 1657 nanocomposite membranes for post-combustion CO_2 capture", ***Journal of Membrane Science***, Vol. 469, (2014), 344-354. https://doi.org/10.1016/j.memsci.2014.06.048

Persian Abstract

چکیده

جداسازی دی اکسید کربن برای محیط زیست ضروری است. استفاده از غشاها برای جداسازی این گاز مقرون به صرفه است، اما ضعف در نفوذپذیری و استحکام مکانیکی مانع تجاری سازی آنها شده است. رابسون ثابت کرد که نفوذپذیری و گزینش پذیری رابطه معکوس دارند و حد بالایی برای جفت گازها ارائه کرد. وی اظهار داشت که هر غشایی که بالاتر از این حد قرار گیرد، قابل تجاری سازی است. دانشمندان برای غلبه بر این مشکل غشاهای ماتریس مخلوط را پیشنهاد کردند. این غشاها شامل دو فاز پلیمری و معدنی هستند. هدف از این تحقیق رفع نقاط ضعف ذکر شده و کسب جایگاه مناسب در نمودار رابسون می باشد. پلیمر Pebax و زئولیت 4A به ترتیب به عنوان فازهای پلیمری و معدنی برای ساخت غشا انتخاب شدند. غشاهای ساخته شده توسط تست های XRD، FT-IR، FE-SEM، BET، EDAX، TGA/DSC و استحکام مکانیکی مورد ارزیابی قرار گرفتند. در نهایت، گزینش پذیری دی اکسید کربن در مقایسه با نیتروژن، اکسیژن و متان به ترتیب ۵۳، ٦٧ و ۷۵ درصد بهبود یافت و موقعیت خوبی در نمودار رابسون به دست آورد.